ACS OMEGA

http://pubs.acs.org/journal/acsodf

Article

Research on the Ability of Bio-rejuvenators to Disaggregate Oxidized Asphaltene Nanoclusters in Aged Asphalt

Xuewen Zheng, Wenyuan Xu,* Haoping Xu, Suxin Wu, and Kai Cao

Cite This: *ACS Omega* 2022, 7, 21736−21749

Read Online

ACCESS | Metrics & More | Article Recommendations

ABSTRACT: A real rejuvenator must have the ability to disaggregate oxidized asphaltene nanoclusters. However, few studies pay attention to the topic, and there is a lack of comparison of the disaggregation ability of different rejuvenators. Thus, the disaggregation ability and regeneration mechanism of three bio-rejuvenators (waste cooking oil (WCO), waste wood oil (WWO), and straw liquefied residue oil (SLRO)) on oxidized asphaltene nanoclusters were studied in this paper. Laboratory tests and molecular dynamics (MD) simulation were used to compare the effectiveness of the three bio-rejuvenators and reveal its corresponding mechanism. It is found that these bio-rejuvenators have a softening effect on aged asphalt binder, but not all of them can disaggregate oxidized asphaltene nanoclusters. The introduction of WWO and WCO can effectively disturb the nanoclusters caused by the increase of polar functional groups during the oxidation process. The effect of WWO is more significant, but neither of them can restore the asphaltene dispersion to the virgin asphalt binder. SLRO has an adverse effect on the disaggregation of oxidized asphaltene nanoclusters. WCO, WWO, and SLRO showed different disaggregation mechanisms, including "pull-out, intercalation, and compression", respectively. WCO and WWO can increase the activation energy reduced by aging in a short aging time, and SLRO makes the activation energy lower. Such findings can help enterprises screen more reasonable rejuvenators to facilitate the recycling of reclaimed asphalt pavement (RAP) materials and promote the sustainable development of the construction industry.

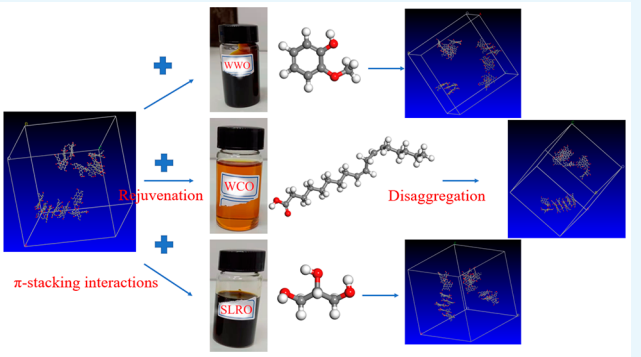

1. INTRODUCTION

Reclaimed asphalt pavement (RAP) contains significant amounts of asphalt binder, and its application in new construction has been promoted as a sustainable practice in the pavement industry and to promote a circular economy. However, this effort has faced challenges such as the aged asphalt's inferior properties compared to the virgin counterpart and its unknown contribution to new pavements. The aged asphalt binder is highly oxidized during the service life. The oxidation of asphaltene molecules is one of the critical factors contributing to the hardening of asphalt and the consequent pavement embrittlement that eventually leads to the deterioration of asphalt's mechanical properties and performance. The major consequence of the irreversible oxidation process is mainly attributed to two factors:[1] first, the evaporation of light asphalt components and the reduction of the maltene/asphaltene phase ratio and second, the oxidation of highly reactive hydrocarbons and polar species that leads to a change in the functional group composition and increased concentration of asphalt's polar components.[2−4] Due to the introduction of polar functional groups in asphaltene molecules, the polar binding forces such as hydrogen bond, van der Waals force, and Coulomb interaction increase, resulting in further molecular agglomeration and the formation of nano-aggregates.[5−7] The nano-aggregation has been implicated in the undesirable high stiffness and brittleness of aged asphalt binder.[8]

To facilitate the recycling and possibly upcycling of aged asphalt binder, there is a need to restore its properties with the help of modifiers referred to as rejuvenators. Rejuvenators are usually divided into two categories: petroleum based and biomass based. Petroleum-based agents are limited in application due to the shortage of petroleum resources.[9] However, a wide range of bio-sources with either animal or vegetal origin can be used to produce bio-oils as renewable rejuvenators. Such bio-rejuvenators can be obtained from various sources such as waste cooking oil (WCO),[10] corn or corn stover,[11−13] castor,[14] wood,[15,16] cashew,[17,18] and swine

Received: March 24, 2022
Accepted: June 1, 2022
Published: June 13, 2022

https://doi.org/10.1021/acsomega.2c01810
ACS Omega 2022, 7, 21736−21749

manure.[19−21] Many studies have evaluated the regeneration performance of bio-rejuvenators from the macroscopic and microscopic perspectives, including mechanical properties,[22,23] rheological properties, fatigue properties, and chemical properties.[24,25] However, little attention has been paid to the deagglomeration of oxidized asphaltene nanoclusters by bio-rejuvenators. It is proved that the ability to properly dissolve and disperse macromolecules and microstructures in aged asphalt binder is the key to the durability and reaging resistance of recycled asphalt.[26,27] Actually, a true rejuvenator should be a kind of asphalt additive that can deagglomerate large asphaltene assemblies into smaller nanoaggregates while replenishing the lost compounds.[28] It is reported that swine manure was effective in restoring oxidized asphalt's thermo-mechanical properties as amide groups in it interact with asphaltene molecules, increasing the stacking distance of asphaltene dimers while changing their conformational packing.[29] From this perspective, the current mainstream of bio-rejuvenators pays little attention to the investigation of disaggregating oxidized asphaltene nanoclusters. And few previous studies compare the disaggregation ability and rejuvenation mechanism of different bio-rejuvenators. Research on the disaggregation behavior of oxidized asphaltene nanoclusters with different rejuvenators can help manufacturers develop and screen rejuvenators that are more suitable for regeneration and eliminate those that are not conducive to regeneration. Therefore, three common bio-oils used in previous studies from WCO,[30,31] straw liquefaction residue (SLRO),[32−34] and waste wood (WWO)[35−37] are selected in this paper to study their disaggregation ability of asphaltene nanoclusters in aged asphalt binder. Computational and experimental methods are used to examine the ability of the three rejuvenators to disaggregate asphaltene clusters. The effect of each bio-rejuvenator on the rheological properties of aged asphalt can be observed through experiments. MD simulation can observe the structural changes of the asphaltene dimer and reveal the regeneration mechanism. In addition, the MD simulation results can be verified by experiments.

2. MATERIALS AND METHODS

2.1. Preparation of Aged Asphalt Binder. In this study, aged 90# asphalt binder is rejuvenated using three bio-rejuvenators: WCO, WWO, and SLRO. The basic properties of the virgin asphalt binder are shown in Table 1.

Table 1. Basic Properties of the Virgin Asphalt Binder

properties	temperature	results
penetration (0.1 mm)	25 °C	82.5
ductility (cm)	15 °C	122
softening point (°C)		47.8

To prepare the aged asphalt binder, the unaged binder was aged initially using a rolling thin-film oven (RTFO) followed by 20 h of aging in a pressure aging vessel (PAV). The aging in the PAV was conducted at 2.10 MPa pressure and at 100 °C temperature for 20 h. And the 20 h PAV aged samples were used to represent long-term aged asphalt.[38] Recycled asphalt was prepared by adding bio-rejuvenators to aged asphalt. The mass of bio-rejuvenators was 10% of the mass of aged asphalt. There are two reasons for choosing the 10% dosage: first, the ability of the three bio-oils to disaggregate asphaltene nanoclusters in aged asphalt is compared under the condition of controlling the same dosage, and second, in previous literature researches, the optimal dosage of the three bio-oils has been mentioned to be about 10%. Although this dosage may not be the optimal dosage of the three bio-rejuvenators in this study, to compare the disaggregation effects of the three rejuvenators under the same research conditions, the dosage was set as 10%. The aged asphalt and bio-rejuvenators were stirred in a 135 °C agitator for 15 min at a stirring rate of 300 rpm to preliminarily achieve the purpose of predispersion. The mixture was then sheared at a high speed of 4000 rpm for 20 min to fully disperse the bio-rejuvenators. After the preparation of the mixture, the samples required for the test were prepared, and the remaining mixture was put into a closed container to prevent pollution for future use.

2.2. Dynamic Shear Rheometer (DSR). An Anton Paar MCR 302 rheometer was used to measure the elastic behavior and viscous behavior of each sample following ASTM D7175. Tests were conducted at 10 °C with frequencies of 0.1−100 rad/s and at a strain rate of 0.1%.[28] For this study, an 8 mm parallel plate spindle was used. Using the corresponding storage modulus (G') and loss modulus (G'') results, the crossover modulus G_c (at which G' is equal to G'') was determined. Additionally, the complex shear modulus (G^*), which is the material deformation resistance with repeated shear, and phase angle (δ), the time lag between stress and strain, were calculated from the measured stress and strain data using eq 1.[28]

$$G^* = \frac{\tau_{max}}{\gamma_{max}} \tag{1}$$

in which

$$\gamma_{max} = \left(\frac{\theta_r}{h}\right) \text{ and } \tau_{max} = \frac{2T}{\pi r^3}$$

where γ_{max} = maximum strain, τ_{max} = maximum stress (Pa), T = maximum applied torque (mN·m), r = radius of the sample (mm), θ = deflection (rotational) angle (°), and h = height of the sample (mm).

2.3. Gas Chromatography−Mass Spectrometry (GC−MS) Test. Gas chromatography−mass spectrometry (GC−MS) analysis was performed using a GCMS-240 instrument from PHARMACIA, Sweden. The chemical constituents of bio-rejuvenators were identified by GC−MS, respectively. For gas chromatography analysis conditions, the initial temperature of the sample was 40 °C and was maintained for 2 min. The temperature was then increased to 290 °C at a heating rate of 4 °C/min and kept for 20 min. Helium gas was selected as the carrier gas at a flow rate of 1.2 mL/min. Under the condition of mass spectrometry, the temperature of the ion source was 260 °C and the temperature of the transmission line was 280 °C. The electron beam energy was 70 eV.

2.4. Molecular Dynamics (MD) Simulation. It has been documented that the asphaltene component increases in most cases after oxidation.[30] The increase of the asphaltene portion is often accompanied by a decrease in the resin and aromatic portion.[16] Besides, due to the reaction of small molecules such as oxygen absorption polymerization and the generation of asphaltene with stronger polarity and higher molecular weight than the virgin asphaltene, which greatly increases the solubility parameters of the total asphaltenes, while the solubility parameters of soft asphalt do not change much, the difference between the solubility parameters of asphaltenes and

https://doi.org/10.1021/acsomega.2c01810
ACS Omega 2022, 7, 21736−21749

soft asphalt becomes larger, and the solubility of soft asphalt to asphaltenes becomes weaker. The main structure of asphaltene is polycyclic aromatic hydrocarbons (PAHs), and the planar aromatic ring system has a strong $\pi-\pi$ force. Due to the aromaticity resulting from the delocalization of π electrons as the responsible factor for the $\pi-\pi$ interaction of asphaltene molecules, an asphaltene layer accumulation structure can be formed and the result is the formation of clusters at the nanoscale.

The continuous oxidation reaction in the long-term aged asphalt binder is considered. More oxygen and sulfur atoms were added to the long-term aged asphalt compared to the virgin asphalt binder.[29] The asphaltene molecule used in this study is the molecular structure published by Martín-Martínez et al.,[39] which has a chemical structure with lower energy and thus provides a more stable and probable model for the asphaltene compared with the original molecule proposed by Li and Greenfield.[40] To develop the model, a system of 15 asphaltene pyrrole molecules shown as "VirAsP" and 15 oxidized asphaltenes[41] shown as "OxAsP" was separately built and optimized (Figure 1).

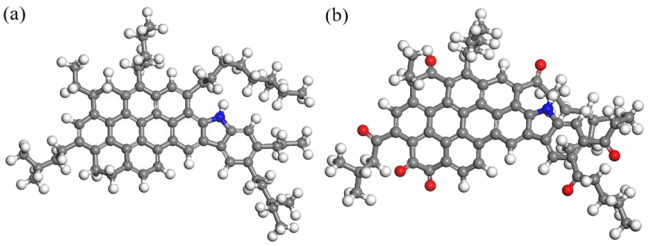

Figure 1. (a) Virgin asphaltene pyrrole (VirAsP) structure and (b) oxidized asphaltene pyrrole (OxAsP) structure.

As can be seen from Tables 2–4, acids, alcohols, and phenols contributed the most to WCO, SLRO, and WWO components, respectively. WCO had the most 9,12-octadecadienoic acid (Z,Z)- (53.4%), SLRO had the most glycerin (10.4%), and WWO had the most 4-ethyl-2-methoxyphenol (9.8%). In this paper, the molecular model with the highest content of three kinds of bio-oils was used as the source oil model when constructing the bio-rejuvenator MD models. Molecular models of the three bio-rejuvenators are shown in Figure 2.

Table 2. The Main Individual Compounds of WCO Identified by GC–MS

	WCO	formula	area (%)
1	9,12-octadecadienoic acid (Z,Z)-	$C_{18}H_{32}O_2$	53.4
2	oleic acid	$C_{18}H_{34}O_2$	22.9
3	*n*-hexadecanoic acid	$C_{16}H_{32}O_2$	9.4
4	7-hexadecyn-1-ol	$C_{16}H_{30}O$	1.9
5	9,17-octadecadienal, (Z)-	$C_{18}H_{32}O$	1.8
6	1,5,9-undecatriene, 2,6,10-trimethyl-, (Z)-	$C_{14}H_{24}$	1.8
7	dibutyl phthalate	$C_{16}H_{22}O_4$	1.7
8	6-octadecenoic acid, methyl ester, (Z)-	$C_{19}H_{36}O_2$	1.6
9	3,4-octadiene, 7-methyl-	C_9H_{16}	1.6
10	cyclopropaneoctanal, 2-octyl-	$C_{19}H_{36}O$	1.4
			97.4%

MD simulation was used to investigate the stacking and aggregation pattern of each model in the presence of the bio-rejuvenator molecules. To do so, each subset of bio-rejuvenators molecules was added to a cell of oxidized asphaltenes at a 10% weight ratio and was solvated in the *n*-heptane solvent.[20] Material Studio was used to carry out the simulation in this study. For aged asphalt and virgin asphalt, when the molecular systems were established, the systems' energy was minimized by the smart method. Then, the systems were run at 800 K for 100 ps in an NVT (constant value for the number of particles, volume, and temperature) followed by an NPT ensemble (constant value for the number of particles, pressure, and temperature) at a pressure of 200 atm and 800 K for 500 ps to shake the system. This will prevent the simulation from sinking into a local minimum energy state. The next procedure began with an NVT ensemble at 408.15 K for 2 ns to reach equilibrium and correct any probable overlaps of molecules. Following an NPT ensemble, the systems were run for 2 ns at a pressure of 1 atm. After the equilibration of oxidized asphaltenes in heptane, the rejuvenator molecules were added to the system. Then, the systems were run at 408.15 K to simulate the mixing temperature of the binder and aggregates in asphalt plants for a typical bio-modified asphalt mix.[20] Although the selected temperature was higher than the boiling point of heptane, the authors deliberately chose it to dilute the solvent enough to reduce its effect on asphaltene aggregation.[41] Then, the systems continued to run in a two-step procedure: a canonical NVT ensemble for 2 ns followed by an isothermal–isobaric NPT ensemble for 2 ns to reach equilibrium. The number of asphaltenes aggregates as well as the average size of aggregates was calculated for each scenario after the systems reached equilibrium.

To have a quantitative measure for the aggregation of asphaltenes, two indices were defined: the number of aggregates and the average size of aggregates. An aggregate was considered as two or more parallel (or near-parallel) sheets being at a distance of less than 4 Å while having at least 50% overlap.[20,42] After the number of aggregates was determined, the average number of aggregates was calculated using the following formula:[20,42]

$$\langle m \rangle = \frac{\sum m N_m}{\sum N_m} \tag{2}$$

where N_m is the number of aggregates containing m asphaltene molecules.

3. RESULTS AND DISCUSSION

3.1. MD Simulation Results. Because aging will increase the proportion of asphaltene, asphaltene tends to aggregate and form nanoclusters under the influence of the $\pi-\pi$ bond. This paper first analyzes the distribution of asphaltene molecules in the virgin asphalt binder and aged asphalt binder and then analyzes the distribution of OxAsp in the presence of bio-rejuvenator molecules so as to analyze the disaggregation ability of the three bio-rejuvenators on OxAsp nanoclusters. To see the relative position of asphaltenes more clearly, after the simulation was completed, the bio-rejuvenator molecules and *n*-heptane molecules were removed, and the side chain of asphaltene molecules was cut off.

Figure 3 shows the distribution state of asphaltenes after the simulation. To qualitatively describe the interaction degree between asphaltenes, the asphaltenes' aggregation in the system is covered with a red shadow. When the red shadow area is larger and the quantity is fewer, it indicates that the

https://doi.org/10.1021/acsomega.2c01810
ACS Omega 2022, 7, 21736–21749

Table 3. The Main Individual Compounds of SLRO Identified by GC−MS

	SLRO	formula	area (%)
1	glycerin	$C_3H_8O_3$	10.4
2	9,12-octadecadienoic acid (*Z*,*Z*)-	$C_{18}H_{32}O_2$	9.2
3	2-linoleoyl-rac-glycerol	$C_{21}H_{38}O_4$	8.7
4	2-monopalmitin	$C_{19}H_{38}O_4$	8.2
5	9-octadecenal, (*Z*)-	$C_{18}H_{34}O$	8.0
6	glyceryl monooleate	$C_{21}H_{40}O_4$	6.7
7	1,3-dioxane, 2-ethyl-5-methyl-	$C_7H_{14}O_2$	4.2
8	hexadecanoic acid, 2-hydroxy-1-(hydroxymethyl)ethyl ester	$C_{19}H_{38}O_4$	4.2
9	oleic acid	$C_{18}H_{34}O_2$	3.1
10	*n*-hexadecanoic acid	$C_{16}H_{32}O_2$	2.2
11	*n*-caprylic acid isobutyl ester	$C_{12}H_{24}O_2$	2.2
12	9,12,15-octadecatrienoic acid, ethyl ester, (*Z*,*Z*,*Z*)-	$C_{20}H_{34}O_2$	2.1
13	10-undecenoyl chloride	$C_{11}H_{19}ClO$	2.0
14	3-(1-azepanyl)-1,2-benzisothiazole 1,1-dioxide	$C_{13}H_{16}N_2O_2S$	1.3
15	3-hexene, (*Z*)-	C_6H_{12}	1.1
			73.6%

Table 4. The Main Individual Compounds of WWO Identified by GC−MS

	WWO	formula	area (%)
1	4-ethyl-2-methoxyphenol	$C_9H_{12}O_2$	9.8
2	guaiacol	$C_7H_8O_2$	6.8
3	3-hydroxy-4-methoxytoluene	$C_8H_{10}O_2$	5.6
4	isoeugenol	$C_{10}H_{12}O_2$	3.8
5	dihydroeugenol	$C_{10}H_{14}O_2$	3.7
6	abieta-8,11,13-triene-19-oic acid	$C_{20}H_{28}O_2$	3.4
7	1-phenanthrenecarboxylicacid	$C_{21}H_{36}O_2$	3.2
8	*p*-cresol	C_7H_8O	2.7
9	7-isopropyl-1-methyl-phenanthrene	$C_{18}H_{18}$	2.4
10	3,5-dimethylphenol	$C_8H_{10}O$	2.1
11	3-methyl-1,2-cyclopentanedione	$C_6H_8O_2$	1.8
12	oleic acid	$C_{18}H_{34}O_2$	1.6
13	*o*-cresol	C_7H_8O	1.6
14	2,7-dimethylphenanthrene	$C_{16}H_{14}$	1.6
15	hydrazinecarboxamide, 2-(1-phenylethylidene)-	$C_9H_{11}N_3O$	1.6
16	phenol	C_6H_6O	1.5
17	3-hydroxy-2-methyl-4-pyrone	$C_6H_6O_3$	1.4
18	catechol	$C_6H_6O_2$	1.4
19	4-methylpyrocatechol	$C_7H_8O_2$	1.2
20	2-methoxy-4-methylphenol	$C_8H_{10}O_2$	1.2
21	benzenamine, 2,2′-(1,2-ethanediyl)bis[*N*,*N*-dimethyl-	$C_{18}H_{24}N_2$	1.2
22	cyclohexanol, 2-[2-pyridyl]-	$C_{11}H_{15}NO$	1.2
			60.8%

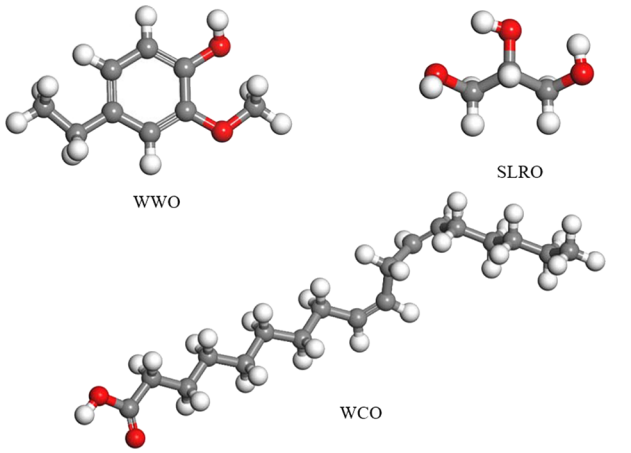

Figure 2. Molecular models of the bio-rejuvenators.

asphaltenes are more aggregated. Comparing Figure 3a,b, it can be clearly seen that VirAsp in the virgin asphalt binder system is distributed in an island shape, the number of red shadows is scattered, and the area is smaller. Most areas are below 100 Å^2, and the largest is about 176 Å^2. In contrast, in the aged asphalt binder system, the red shadow area is larger and the number is fewer. The areas are up to more than 300 Å^2, indicating that the VirAsp molecules are evenly distributed, and the interaction between them is weak. Thus, large-area aggregation is not formed. Meanwhile, the OxAsp molecules in the aged asphalt binder are concentrated, indicating that the interaction between them is more intense, and nanoclusters are formed.

Figure 4a−c respectively shows the distribution of OxAsp in the presence of bio-rejuvenators. Among the three systems, the OxAsp distribution with WWO is the most dispersed, presenting a multipoint dispersion state. However, compared with the virgin asphalt, there is still a large area of red shadow in the system. The value is basically the same as that of aged asphalt, with an area of more than 300 Å^2, indicating that there is still a relatively dense asphaltene aggregation in the system. WCO followed with good dispersion, and the worst is the asphalt binder system with SLRO. Similarly, the maximum shadow area in the two systems is almost the same as that of aged asphalt. However, after the addition of SLRO, the OxAsp interaction almost has no difference from that of the aged asphalt system, indicating that SLRO has a limited ability to disaggregate OxAsp nanoclusters.

To see the distribution of asphaltene more clearly, the snapshots after the simulation are shown in Figures 5 and 6. Figure 5a shows that due to the interaction between VirAsp molecules, some VirAsp molecules are stacked in parallel, which is caused by the $\pi-\pi$ interaction and hydrogen bonding caused by the structural characteristics of the large aromatic ring system and heteroatoms of asphaltene molecules.[43] The stacking structure is more dense in Figure 5b. The OxAsp molecular sheet is changed from the original two- or three-sheet stacking to the stacking form of three or more sheets, and

https://doi.org/10.1021/acsomega.2c01810
ACS Omega 2022, 7, 21736−21749

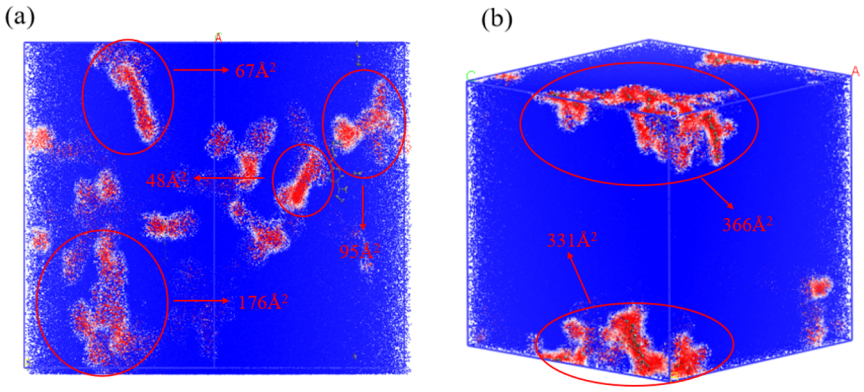

Figure 3. Asphaltene distribution state: (a) virgin asphalt and (b) aged asphalt.

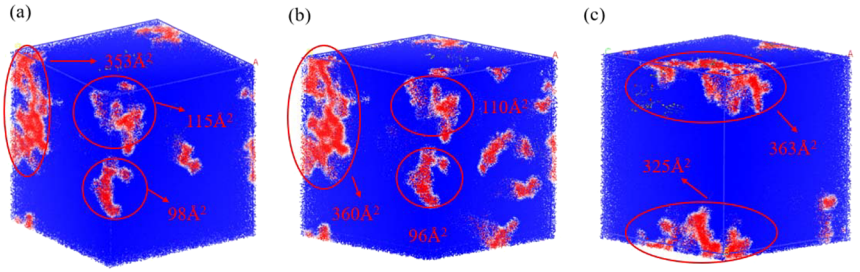

Figure 4. Asphaltene distribution state: (a) WCO, (b) WWO, and (c) SLRO.

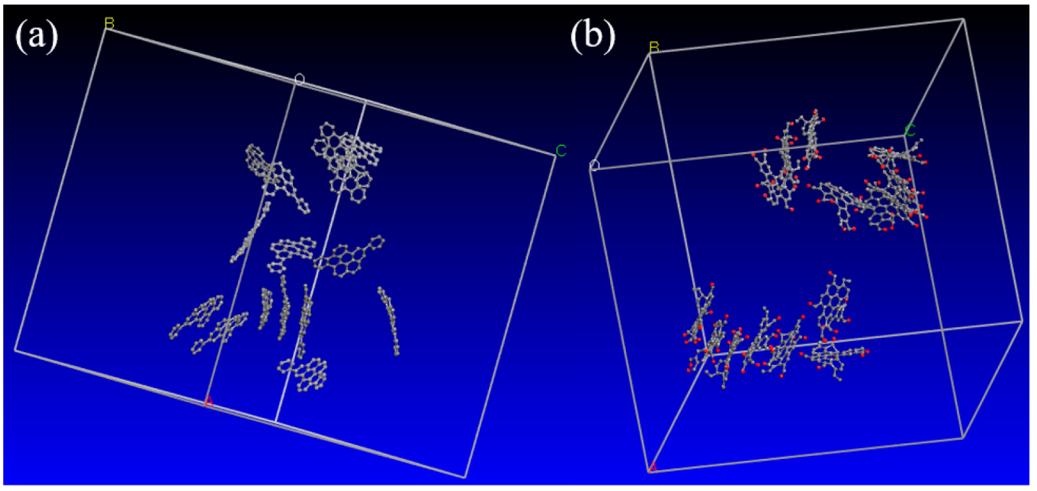

Figure 5. Asphaltene stacking form: (a) virgin asphalt and (b) aged asphalt.

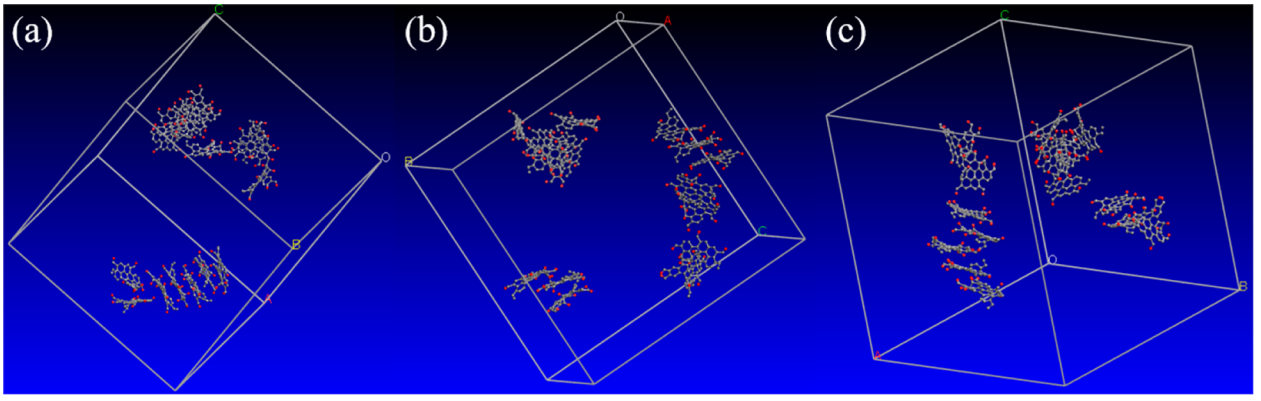

Figure 6. OxAsp stacking form: (a) WCO, (b) WWO, and (c) SLRO.

https://doi.org/10.1021/acsomega.2c01810
ACS Omega 2022, 7, 21736−21749

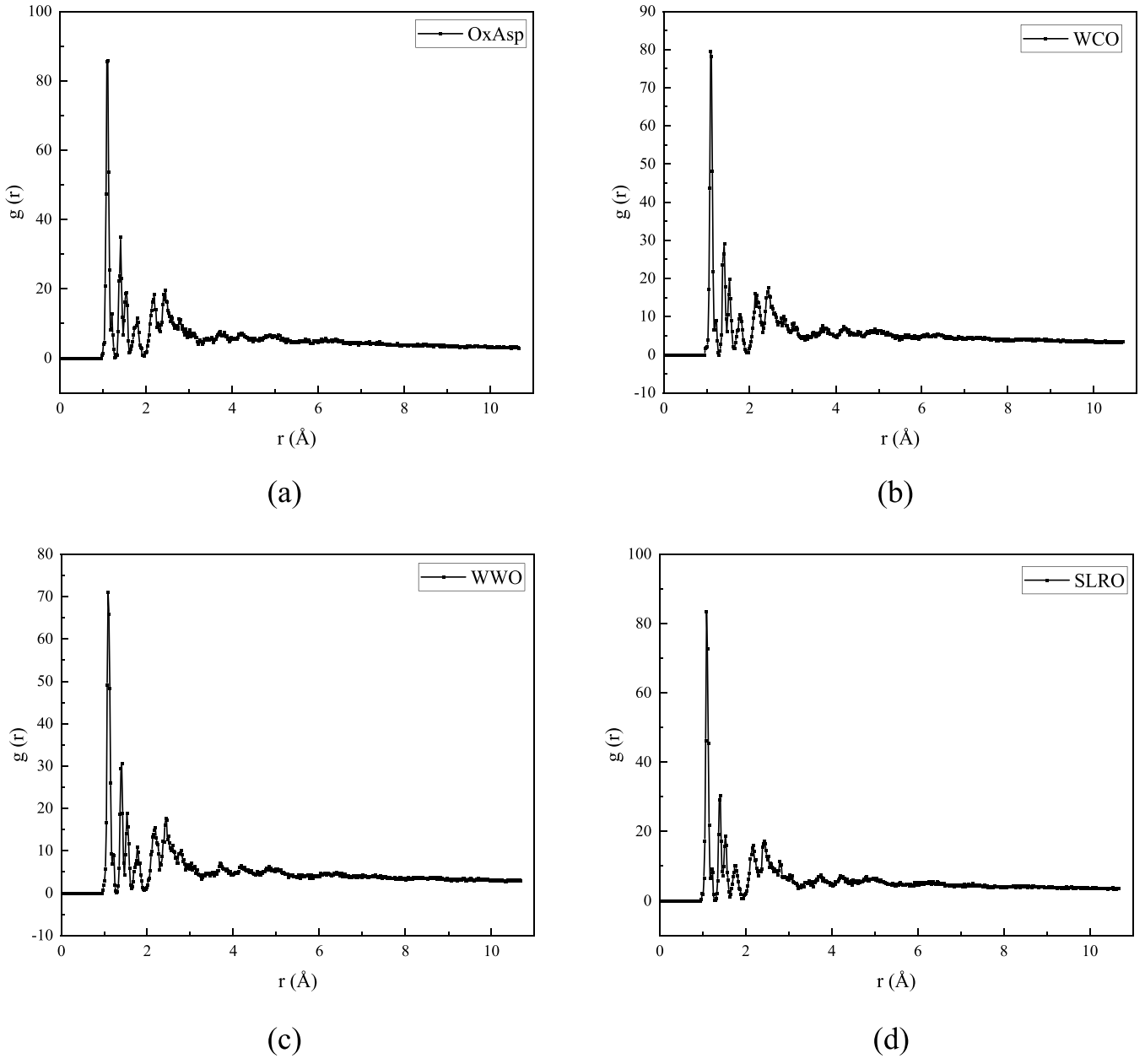

Figure 7. RDF between asphaltenes: (a) OxAsp, (b) WCO, (c) WWO, and (d) SLRO.

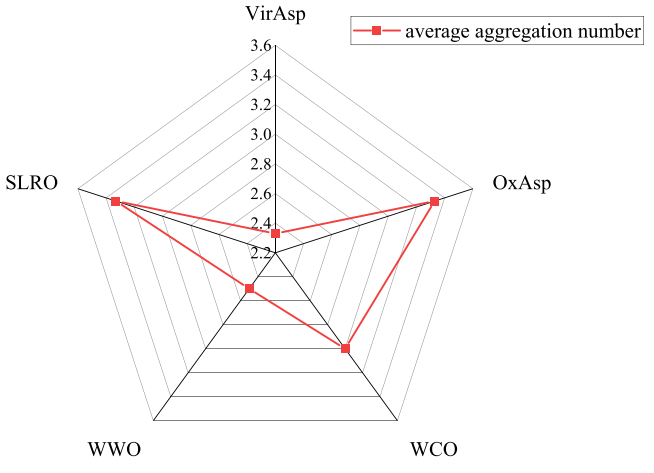

Figure 8. Average aggregate number of asphaltene slices.

the maximum number of stacked sheets can reach five. It is reported the $\pi-\pi$ interaction between asphaltene molecules reaches the maximum when they are parallel to each other,[44] indicating that the distribution is more concentrated than that in the virgin asphalt binder. This is due to the increase of oxygen-containing polar functional groups after asphalt aging, which promotes the interaction of asphaltene and forms nano-aggregation. Figure 6 shows the OxAsp stacking structure after adding bio-rejuvenators. In the presence of WCO and SLRO, there is a common focus; that is, the maximum number of oxidized asphaltene stacks is five, which is consistent with the aged asphalt, indicating that the two bio-rejuvenators have a weak disaggregation ability for larger oxidized asphaltene nanoclusters. WWO can split the five-sheet stacking into two- and three-sheet stacking, showing a strong ability to disaggregate larger oxidized asphaltene nanoclusters. In Figure 6a, WCO divides the three-sheet stacking in the system into two- and one-sheet stacking, which alleviates the aggregation of

https://doi.org/10.1021/acsomega.2c01810
ACS Omega 2022, 7, 21736−21749

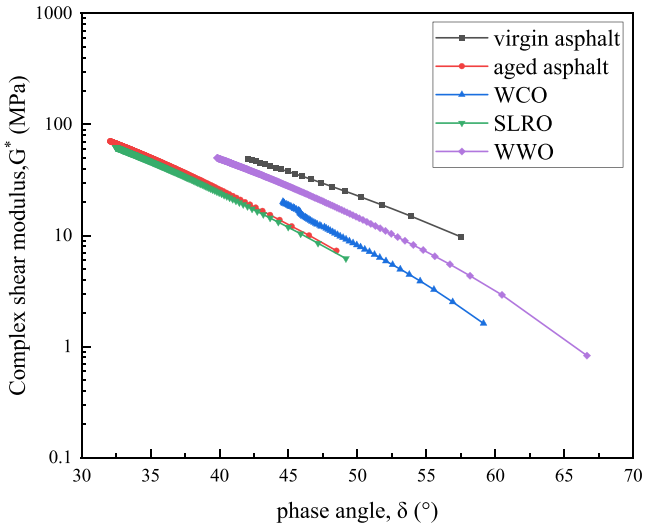

Figure 9. Complex shear modulus G^* and phase angle δ.

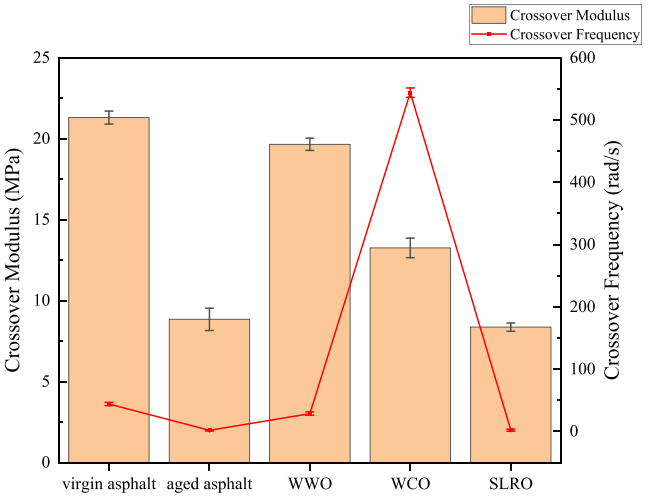

Figure 10. Crossover modulus and frequency.

OxAsp. In Figure 6b, in addition to decomposing the five-sheet stacking, there are three three-sheet stacking structures in the system, and the number of stacking is higher than that of virgin asphalt. In the presence of SLRO (Figure 6c), the stacking structures in the system have hardly changed, indicating that SLRO is hardly effective in alleviating oxidized asphaltene accumulation.

To quantitatively describe the aggregation degree of asphaltene in the MD model system, the radial distribution function (RDF) between asphaltenes is introduced for evaluation, as shown in Figure 7. RDF is an important method to analyze the internal structure of organic polymer materials. The basic principle of RDF is to calculate the probability of the occurrence of other molecules around the reference molecule. As can be seen from Figure 7, the RDF of all asphalt systems reaches the maximum value in the range of 0−3 Å, and the number of peaks in this range is the same, indicating that the relative distribution of oxidized asphaltene in all asphalt systems is basically unchanged. However, the highest RDF values of all systems are different, indicating that the aggregation quantity of oxidized asphaltene is different. The aggregation of oxidized asphaltene is more serious in the system with a high peak value. The peak values of RDF in both the aged asphalt binder and SLRO asphalt binder are above 80. WWO and WCO can reduce the peak values, and WWO reduces the peak values to about 70, which is the most significant. It shows that both WCO and WWO can alleviate the agglomeration of OxAsp. The effect of WWO is better, and SLRO has the worst effect.

To further quantitatively evaluate the disaggregation ability of the three bio-rejuvenators on oxidized asphaltene nanoclusters, the average aggregation number of asphaltenes in each system is calculated according to formula 2. The high dispersion of asphaltenes can be characterized by the small average aggregate number. It can be seen from Figure 8 that the average aggregation number in VirAsp is 2.33, while that of OxAsp is 3.33, which is increased by 42.9% compared with that of VirAsp. It indicates that asphaltenes are evenly distributed before asphalt binder aging. After aging, due to the action of polar functional groups, the original asphaltene slices aggregate into larger asphaltene clusters. After WCO and WWO are added, the OxAsp average aggregate numbers are 3 and 2.5, respectively, which decreased by 9.91 and 24.92% compared with aged asphalt binder, indicating that WCO and WWO could decompose oxidized asphaltene clusters into smaller aggregation. The addition of SLRO does not change the average aggregation amount of OxAsp, which is equivalent to that of the aged asphalt system, indicating that SLRO has no ability to disaggregate oxidized asphaltene clusters. The ability to disaggregate oxidized asphaltene clusters is WWO > WCO > SLRO.

3.2. DSR Test Results. To verify the accuracy of MD simulation, DSR test results were used for verification in this section. In fact, when describing the molecular weight of a polymer, previous studies prefer to use the GPC test for evaluation. However, according to the report of Wang et al., the GPC test has two defects:[45] First, because GPC samples need to be filtered before entering the column, some large microstructures formed during aging may not pass through the filter paper and will not be counted. However, the large microstructure is the key to evaluate whether the rejuvenators can effectively dissolve the aged products. Second, the microstructure of GPC is affected by the solvation ability of the solvent. Therefore, even through the microstructure of GPC filter, due to the different solvation capacity of maltenes and GPC solvents, their size may be different from that existing in the asphalt binder. In this paper, the frequency scanning mode was used to evaluate the cross modulus, which is the corresponding value at which shear storage modulus (G') and shear loss modulus (G'') have the same magnitude. The crossover point is defined by two symbols of the crossover frequency and the crossover modulus. At this point, there is a transition from liquid to solid materials. The polydispersity of polymers and bitumen has been reported to be associated with the cross modulus.[46] Polydispersity index (PDI) in rheology is usually defined as 100,000/cross modulus, where the cross modulus is expressed in pascals. Although the molecular structure of asphalt differs from that of polymers, its asphaltene portion (heptane insoluble) is the focus of this paper and consists of self-assembled nanoaggregates with a molecular weight of approximately 980 g/mol and size of few nanometers.[21,47] PDI is also associated with the point at which sol−gel transfer occurs in asphaltene-rich bitumen.[48,49] Farrar et al. used the Christensen and Anderson model for bitumen, referred to as the dispersed polar fluid model, for utilizing the crossover modulus as a parameter related to the

https://doi.org/10.1021/acsomega.2c01810
ACS Omega 2022, 7, 21736−21749

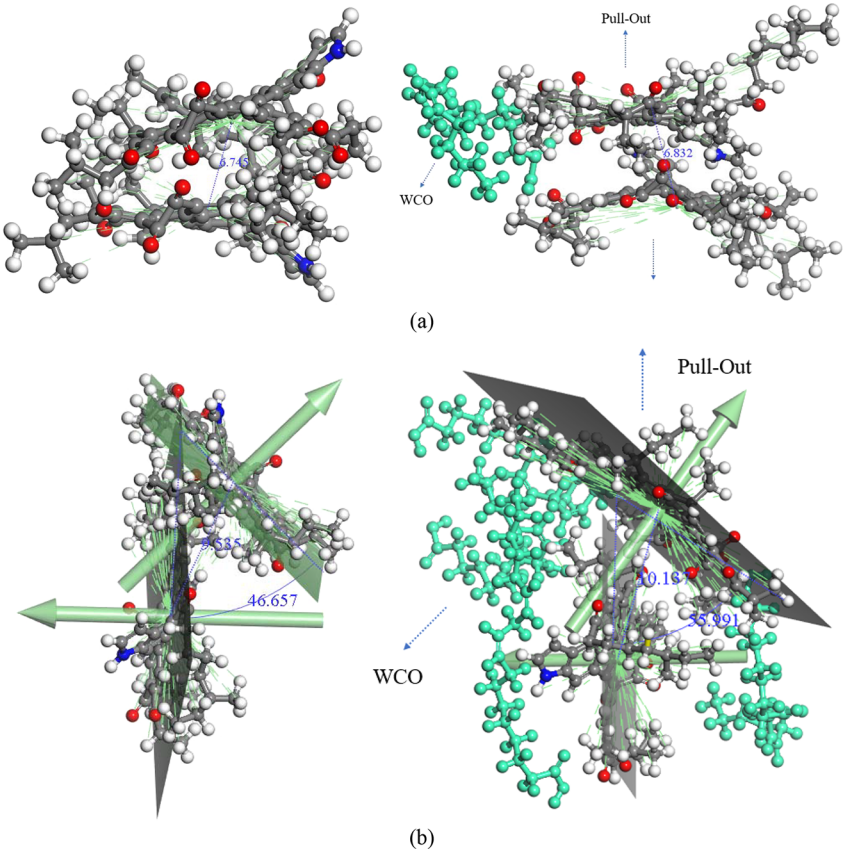

Figure 11. Effect of WCO on the microstructure of OxAsp: (a) offset face-to-face stacking and (b) T-shaped stacking. Note: green molecules for WCO.

asphalt structure and its evolution with aging. They found an approximate linear relationship between oxygen uptake and the logarithmic reciprocal of the crossover modulus.[46] Liu et al. studied the evolution of asphalt during oxidative aging and used the change of crossover value as an index of the aging process. They found that, with the increase of aging time, the crossover modulus of virgin asphalt and modified asphalt continued to decline.[50] As aging progresses, the number of polar functional groups in bitumen increases, leading to intermolecular interactions that lead to asphaltene aggregation. This, in turn, promotes the formation of nanoaggregates of different sizes, as molecular affinity overlays the oxidized asphaltene hydrophilic side chains that form during aging. The different nano-aggregation will increase the polydispersity of the asphalt matrix. Previous studies show that almost all rejuvenators can increase the cross frequency of aged asphalt, affect the viscous composition of aged asphalt, and play a role in softening aged asphalt binder, but not all rejuvenators can increase the cross modulus of aged asphalt binder,[25] which is an indicator to measure the degree of polydispersity.[51−53] The polydispersity of asphaltenes is reported to increase with aging, and the polydispersity is inversely proportional to the cross modulus.[28,51] Thus, the appropriate rejuvenators to disaggregate or disperse asphaltene clusters will increase the cross modulus of aged asphalt binder.

Through the DSR test results, the cross modulus and cross frequency of aged asphalt binder in the presence of the three bio-rejuvenators are compared to analyze the dispersion ability of the three bio-rejuvenators on oxidized asphaltene nanoclusters. Figure 9 shows that aging increases the composite shear modulus and reduces the range of the phase angle. Except for SLRO, the other two kinds of bio-rejuvenators can reduce the modulus value and enlarge the phase angle threshold, indicating that WWO and WCO can improve the rheological properties of aged asphalt. However, SLRO exerts poor regeneration performance for making the modulus and phase angle equal to those of aged asphalt. When the storage modulus G' and the loss modulus G'' are equal, the corresponding modulus is the cross modulus. Figure 10 shows the cross modulus and cross frequency of several asphalt binders. The results show that compared with virgin asphalt, the cross modulus and cross frequency of aged asphalt are reduced by 58.5 and 96%, respectively. Three bio-rejuvenators can increase the cross frequency of aged asphalt. The most obvious is WCO followed by WWO and finally SLRO. It is worth noting that the cross frequency of aged asphalt with WCO is much higher than that of virgin asphalt binder, but the cross frequency value after adding WWO and SLRO cannot reach the value of virgin asphalt, indicating that WCO has an excellent softening effect. However, not all bio-rejuvenators can increase the cross modulus. WWO recovers the cross modulus by about 92.3% followed by WCO, and SLRO is the worst in improving the cross modulus. However, even WWO cannot restore the cross modulus of aged asphalt. For example, SLRO even reduces the cross modulus. The above research conclusions show that WWO is more talented in disaggregating asphaltene clusters and WCO is more suitable as a softener of aged asphalt. The DSR test results are consistent with the MD simulation results, which verify the accuracy of the MD simulation results.

https://doi.org/10.1021/acsomega.2c01810
ACS Omega 2022, 7, 21736−21749

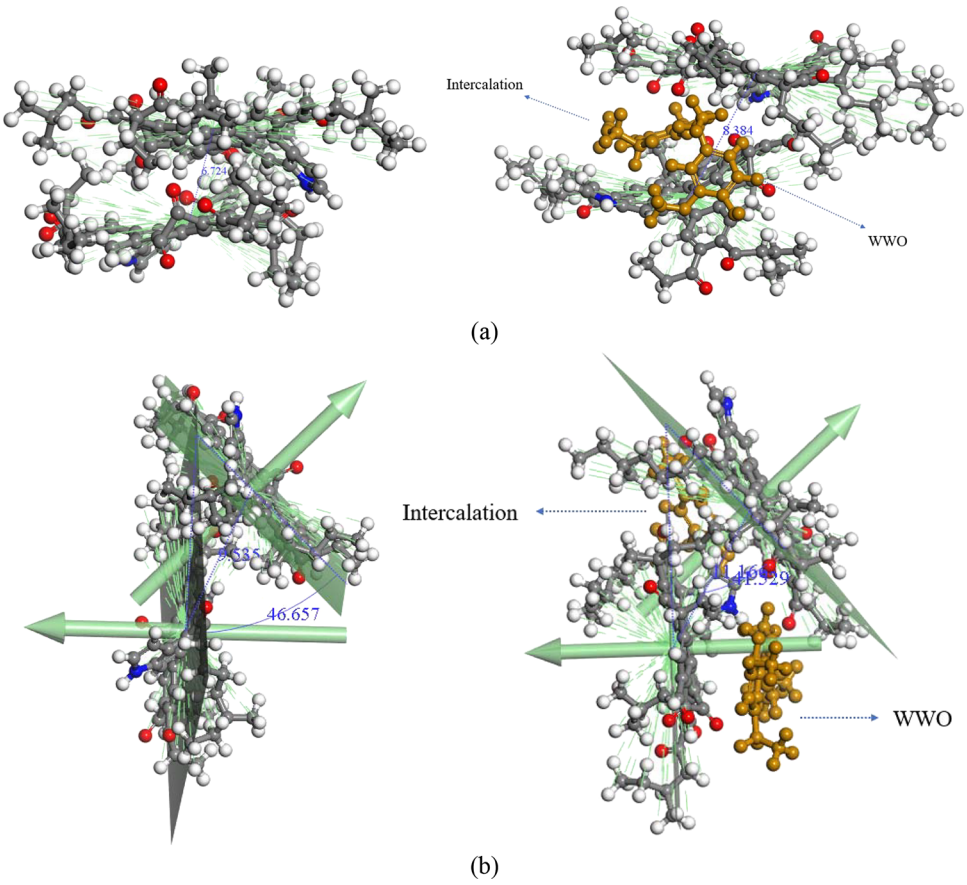

Figure 12. Effect of WWO on the microstructure of OxAsp: (a) face-to-face stacking and (b) T-shaped stacking. Note: brown molecules for WWO.

3.3. Effect of Bio-rejuvenators on the Micromorphology of Oxidized Asphaltene. To understand the regeneration mechanism of three kinds of bio-rejuvenators on aged asphalt, the micromorphology of oxidized asphaltene in the same position in their respective systems in the presence or absence of bio-rejuvenators is studied by MD simulation. Figures 11−13 show the micromorphology of oxidized asphaltenes under different conditions. Oxidized asphaltenes mainly have the following stacking structures: face-to-face stacking, offset face-to-face stacking, T-shaped stacking, and other aggregation phenomena, which are basically consistent with the previous research conclusions.[29,41,43,54] It is reported that aging increases the polar functional groups, which increases the strength of mutual attraction between molecules and shortens the distance between PAH structures and makes it easier to stack.

Figure 11 shows the stacking morphology of OxAsp before and after adding WCO. For the aged asphalt binder, the molecular centroid distances of asphaltenes in offset face-to-face stacking (Figure 11a, left side) is 6.745 Å. In T-shaped stacking (Figure 11b, left side), the centroid distance between the two OxAsp molecules is 9.535 Å with an angle of 46.657°. WCO molecules play a ″pull-out″ role between OxAsp molecules in offset face-to-face (Figure 11a, right side) and T-shaped stacking (Figure 11b, right side). When the WCO molecules approach the asphaltene dimer, OxAsp molecules move in the opposite direction, increasing the centroid distance from 6.745 to 6.832 Å. In T-shaped stacking, the centroid distance and included angle of the two OxAsp molecules increase from 9.535 Å and 46.657° to 10.137 Å and 55.991°, respectively. It can be seen that the disaggregation ability of WCO to OxAsp molecules in offset face-to-face stacking is not as strong as that in T- shaped stacking. This may be due to the fact that the OxAsp interactions are stronger in offset face-to-face stacking structures compared to T-shaped stacking.

WWO molecules show an ″intercalation″ effect in OxAsp aggregates. The ″intercalation″ effect of WWO is achieved by interfering with the $\pi-\pi$ interaction between aromatic nuclei in OxAsp molecules. WWO separates aromatic nuclei from each other to increase interstitial distance. In Figure 12a (right side), WWO is embedded in OxAsp aggregates, increasing the gap between the two PAH planes. In face-to-face stacking, the ″intercalation″ regeneration mode reduces the agglomeration of OxAsp molecules, and the distance of the OxAsp centroid increases from 6.724 to 8.384 Å. For T-shaped stacking (Figure 12b, right side), when WWO is close to PAHs, the strong repulsion causes the upper OxAsp molecule to move away from the WWO molecule along the direction perpendicular to the plane of the WWO molecule. At the same time, affected by the attraction of the lower OxAsp, the upper OxAsp tends to approach downward, but affected by the repulsion of another WWO molecule, the two OxAsp molecules cannot approach. This explains why the centroid distance and included angle of two OxAsp molecules range from 9.535 to 11.166 Å and 46.657 to 41.529°, respectively.

Figure 13 shows that when SLRO is added to the aged asphalt binder, the aggregation of OxAsp is more serious in offset face-to-face stacking. In this scenario, SLRO molecules are basically at the periphery of OxAsp aggregates and show a

https://doi.org/10.1021/acsomega.2c01810
ACS Omega 2022, 7, 21736−21749

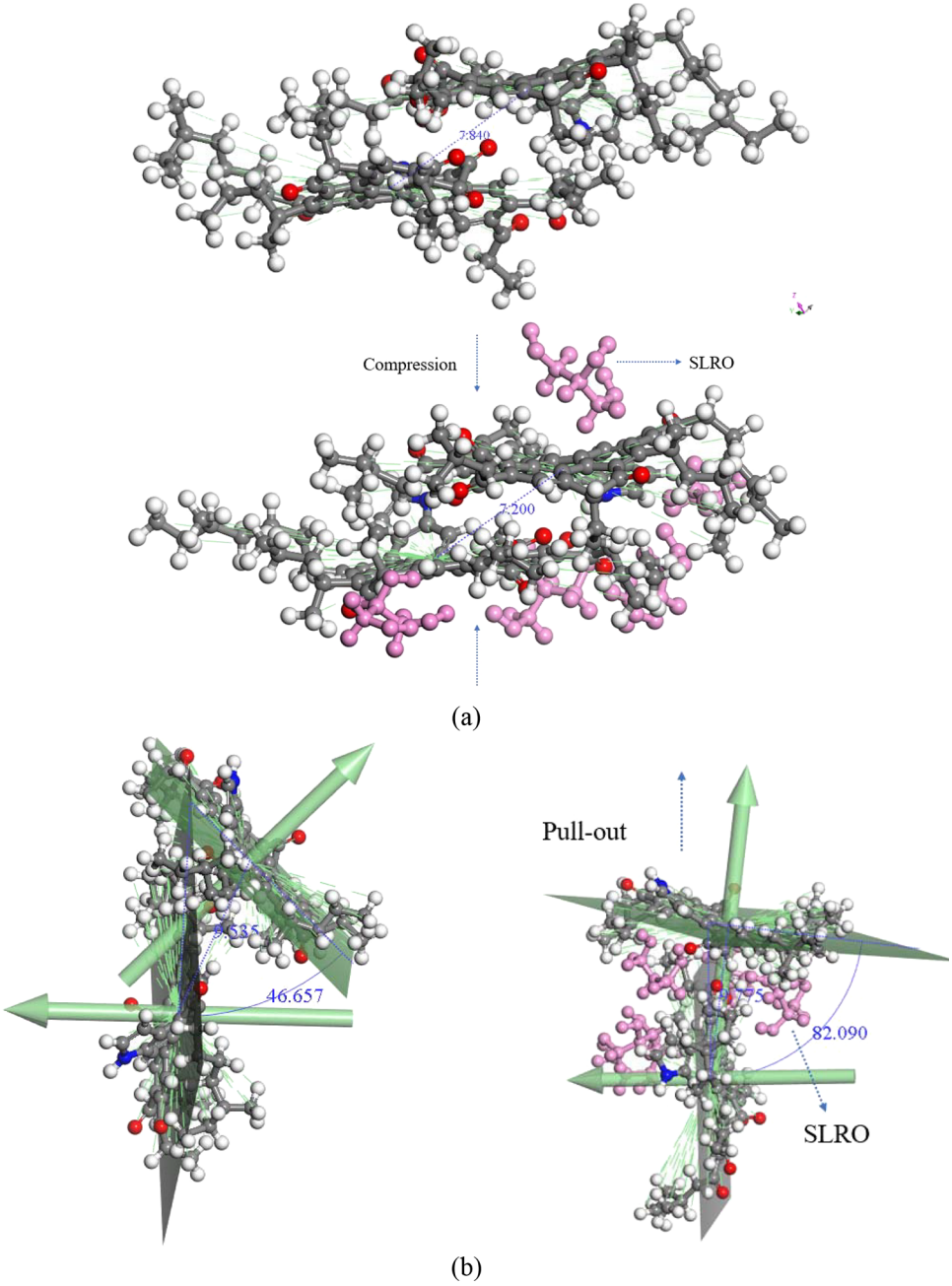

Figure 13. Effect of SLRO on the microstructure of OxAsp: (a) offset face-to-face stacking and (b) T-shaped stacking. Note: purple molecules for SLRO.

″compression″ effect. In the offset face-to-face stacking (Figure 13a), the centroid distances of OxAsp molecules decrease from 7.840 to 7.200 Å, which means that when SLRO is close to OxAsp aggregates, there is a strong repulsion force between SLRO molecules and OxAsp molecules, which promotes the closer distance of OxAsp molecules. However, in T-shaped stacking (Figure 13b), SLRO exerts a ″pull-out″ effect, and the centroid distance and included angle slightly increase from 9.535 Å and 46.657° to 9.775 Å and 82.090°, respectively. This means that SLRO has the ability to slightly alleviate the T-shaped aggregation of OxAsp molecules, but this ability is weak and only works in the state of T-shaped accumulation. However, there is less T-shaped accumulation in aged asphalt, so the regeneration ability of SLRO is poor.

3.4. Interaction between the OxAsp Molecules in the Presence of Bio-rejuvenators. To understand how bio-rejuvenators reduce the negative effects of aging on molecular conformation, especially on oxidized asphaltene aggregates, the interactions between oxidized asphaltene and the main components of bio-rejuvenators were studied. Figure 14 shows the intermolecular binding energy, the binding distance (d), and its variations (Δd) between OxAsp molecules in the presence and absence of bio-rejuvenators. The results show that SLRO enhances the force between oxidized asphaltenes and reduces the binding distance between them in offset face-to-face stacking. However, SLRO slightly increases the binding distance while enhancing the force between oxidized asphaltenes. WCO and WWO can weaken the forces between the oxidized asphaltenes and increase the binding distance.

https://doi.org/10.1021/acsomega.2c01810
ACS Omega 2022, 7, 21736−21749

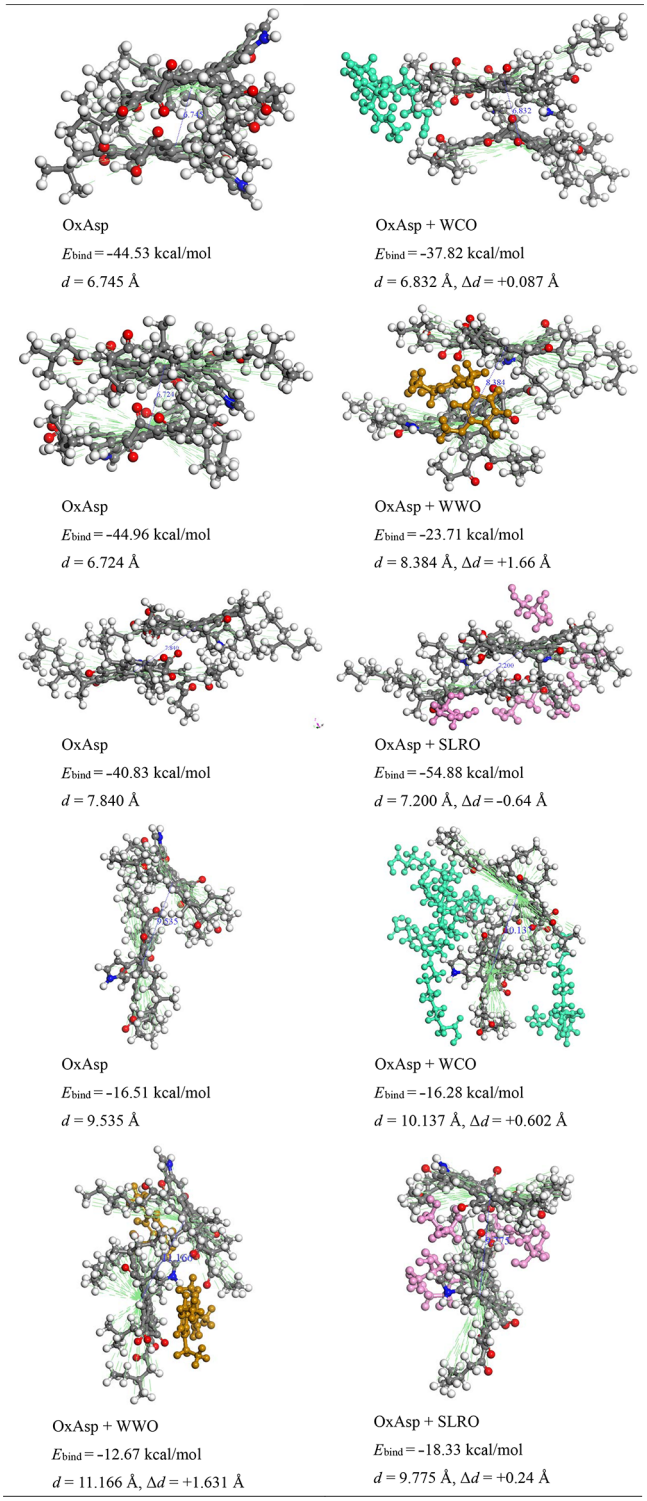

Figure 14. Interactions between OxAsp molecules in the presence of bio-rejuvenators.

Comparing the same kind of stacking, for example, in T-shaped stacking, affected by the "intercalation" effect, the force between oxidized asphaltenes is the weakest, and the binding distance is the largest in the presence of WWO, indicating that WWO has the best disaggregation ability for oxidized asphaltene aggregates followed by WCO. This is consistent with the evaluation results of the DSR test.

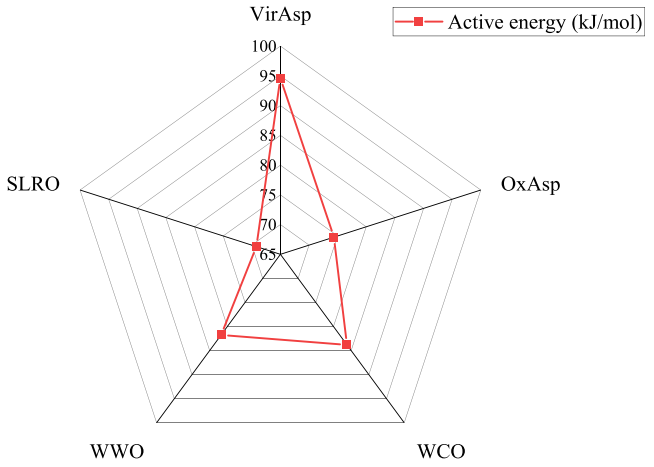

Figure 15. Active energy results.

3.5. Active Energy Results. The concept of activation energy was first proposed by Eyring in 1936 and is mainly used to describe flow barriers.[55] Based on the correlation between the activation energy and the $G^*/\sin\delta$ parameter, asphalt binders with higher activation energy have greater viscosity at higher temperatures than asphalt binders with lower activation energy. The activation energy of asphalt binders containing recycled asphalt binders was investigated by Jamshidi et al.[56] The results show that compared to neat asphalt binders, recycled asphalt binders (which are highly aged) require more energy to overcome intermolecular resistance. In this paper, the effects of three bio-rejuvenators on the activation energy of aged asphalt are studied. The activation energy can be calculated based on the Arrhenius equation (eq 3).

$$\eta_a = A\exp(E_\eta/RT) \tag{3}$$

where η_a = viscosity (Pa · s), A = pre-exponential factor (dimensionless constant), E_η = active energy (kJ/mol), R = gas constant [8.314 J/(mol·K)], and T = temperature (K).

Figure 15 shows the activation energy of virgin asphalt, aged asphalt, and aged asphalt after adding bio-rejuvenators. As can be seen from Figure 15, different from previous studies, the activation energy of aged asphalt does not increase. In this paper, the activation energy of aged asphalt is significantly lower than that of virgin asphalt, and the activation energy of virgin asphalt is the highest among several asphalts. The activation energy of aged asphalt after adding three bio-rejuvenators is also lower than that of virgin asphalt. Compared with the asphalt with bio-rejuvenators, the activation energy of the asphalt with SLRO is the smallest, even lower than that of the aged asphalt, while WWO and WCO can increase the activation energy of the aged asphalt by basically the same range, and the improvement degree of WCO is slightly higher than that of WWO. It should be noted that the decrease of aromatics and resins during aging and the subsequent increase of asphaltene are related to the increase of the polarity of the former substance so that they become insoluble enough to be separated in heptane. This in turn leads to an increase in the percentage of total weight of so-called asphaltenes in aged bitumen. However, the average molecular weight of these new classes is lower than that of the original asphaltenes, suggesting that some resins and aromatics are added to asphaltenes due to aging.[57] Generally, the increased polarity promotes intermolecular interactions and the formation of asphaltene nano-

https://doi.org/10.1021/acsomega.2c01810
ACS Omega 2022, 7, 21736−21749

aggregates, which can easily shear against each other and may cause a reduction in activation energy at a low aging time.[12] This can explain the reduction in the activation energy of aged asphalt. It further shows that WCO and WWO can effectively alleviate the reduction of activation energy and alleviate the aggregation of oxidized asphaltene, while SLRO has no effect.

4. CONCLUSIONS

Asphalt aging is inevitable, which changes the chemical composition and molecular structure of the asphalt binder and promotes the formation of asphaltene clusters. The disaggregation of oxidized asphaltene nanoclusters by three bio-rejuvenators (WCO, WWO, and SLRO) is studied. MD simulation and DSR test are used to check whether the rejuvenators could disaggregate asphaltene nanoclusters, and the regeneration mechanism is analyzed. The conclusions are as follows:

1. MD simulation shows that WWO significantly reduces the aggregation size of oxidized asphaltenes by increasing the dispersion of oxidized asphaltenes. WCO is not as capable as WWO in this aspect, while SLRO not only fails to solve oxidized asphaltene nanoclusters but also makes the aggregation of oxidized asphaltenes more serious.
2. According to the results of rheological properties, such as cross modulus and cross frequency, SLRO can only soften aged asphalt binder, while WWO and WCO activate the viscous and elastic components of aged asphalt binder, which is manifested by an increase in the cross modulus and cross frequency. WWO increases the crossover modulus more significantly, while WCO increases the crossover frequency more obviously.
3. During the process of disaggregating oxidized asphaltene clusters, WCO shows a ″pull-out″ effect. This effect is more effective in alleviating T-shaped stacking and general in offset face-to-face stacking. WWO exerts an ″intercalation″ effect in the process of oxidized asphaltene nanocluster disaggregation. There is a strong repulsive force between WWO and oxidized asphaltene molecules, which causes the oxidized asphaltene molecules to move backward and increase the distance between PAHs so as to achieve the effect of oxidized asphaltene nanocluster disaggregation. SLRO shows a ″compression″ effect in offset face-to-face stacking and relatively weak ″pull-out″ effect in T-shaped stacking. The ″compression″ effect makes the distance between oxidized asphaltenes closer.
4. After aging, the polar components of asphalt increase, which make it easier to shear between aggregated particles in a short time of aging and reduce the activation energy of asphalt. Both WCO and WWO can improve the activation energy of aged asphalt, but SLRO makes the activation energy of aged asphalt lower, indicating that WCO and WWO can alleviate the aggregation of asphaltene to a certain extent.
5. The research in this paper is based on the *n*-heptane environment. Although it does not affect the reliability of the results, it is different from the real asphalt system. The disaggregation effect of rejuvenators on oxidized asphaltene nanoclusters in the real asphalt system should be further studied.

AUTHOR INFORMATION

Corresponding Author

Wenyuan Xu − *School of Civil Engineering, Northeast Forestry University, Harbin 150040, China*; orcid.org/0000-0002-1397-9305; Email: xuwenyuan@nefu.edu.cn

Authors

Xuewen Zheng − *School of Civil Engineering, Northeast Forestry University, Harbin 150040, China*

Haoping Xu − *School of Civil Engineering, Northeast Forestry University, Harbin 150040, China*

Suxin Wu − *School of Civil Engineering, Northeast Forestry University, Harbin 150040, China*

Kai Cao − *College of Civil Engineering and Architecture, Zhejiang University, Hangzhou 310058, China*

Complete contact information is available at: https://pubs.acs.org/10.1021/acsomega.2c01810

Author Contributions

Xuewen Zheng: conceptualization, methodology, investigation, writing − original draft. Kai Cao: validation, software, formal analysis, visualization. Haoping Xu: testing and analyzing data, formal analysis. Suxin Wu: testing and analyzing data. Wenyuan Xu: resources, writing − review & editing, supervision, data curation.

Notes

The authors declare no competing financial interest.

ACKNOWLEDGMENTS

The authors are grateful for the financial support by the scientific and technological projects of the Department of Transportation of Heilongjiang Province (2019HLJ0012).

REFERENCES

(1) Lesueur, D. The colloidal structure of bitumen: consequences on the rheology and on the mechanisms of bitumen modification. *Adv. Colloid Interface Sci.* **2009**, *145*, 42−82.

(2) Hofko, B.; Eberhardsteiner, L.; Füssl, J.; Grothe, H.; Handle, F.; Hospodka, M.; Grossegger, D.; Nahar, S. N.; Schmets, A. J. M.; Scarpas, A. Impact of maltene and asphaltene fraction on mechanical behavior and microstructure of bitumen. *Mater. Struct.* **2016**, *49*, 829−841.

(3) Handle, F.; Harir, M.; Füssl, J.; Koyun, A. N.; Grossegger, D.; Hertkorn, N.; Eberhardsteiner, L.; Hofko, B.; Hospodka, M.; Blab, R.; Schmitt-Kopplin, P.; Grothe, H. Tracking Aging of Bitumen and Its Saturate, Aromatic, Resin, and Asphaltene Fractions Using High-Field Fourier Transform Ion Cyclotron Resonance Mass Spectrometry. *Energy Fuels* **2017**, *31*, 4771−4779.

(4) Le Guern, M.; Chailleux, E.; Farcas, F.; Dreessen, S.; Mabille, I. Physico-chemical analysis of five hard bitumens: Identification of chemical species and molecular organization before and after artificial aging. *Fuel* **2010**, *89*, 3330−3339.

(5) Samieadel, A.; Oldham, D.; Fini, E. H. Investigating molecular conformation and packing of oxidized asphaltene molecules in presence of paraffin wax. *Fuel* **2018**, *220*, 503−512.

(6) Redelius, P.; Soenen, H. Relation between bitumen chemistry and performance. *Fuel* **2015**, *140*, 34−43.

(7) Dickie, J. P.; Yen, T. F. Macrostructures of the asphaltic fractions by various instrumental methods. *Anal. Chem.* **1967**, *39*, 1847−1852.

(8) Wang, Y.; Zhao, K.; Li, F.; Gao, Q.; Lai, K. W. C. Asphaltenes in asphalt: Direct observation and evaluation of their impacts on asphalt properties. *Constr. Build. Mater.* **2021**, *271*, No. 121862.

(9) Xu, M. *Design and Performance Verifcation of Rejuvenator Based on Molecular Difusion Fusion Mechanism*; Harbin Institute of Technology 2019.

(10) Ahmed, R. B.; Hossain, K. Waste cooking oil as an asphalt rejuvenator: A state-of-the-art review. *Constr. Build. Mater.* **2020**, *230*, No. 116985.
(11) Dong, Z.-J.; Zhou, T.; Wang, H.; Luan, H. Performance Comparison between Different Sourced Bioasphalts and Asphalt Mixtures. *J. Mater. Civ. Eng.* **2018**, *30*, No. 04018063.
(12) Zhou, T.; Kabir, S. K. F.; Cao, L.; Fini, E. H. Effects of ultraviolet exposure on physicochemical and mechanical properties of bio-modified rubberized bitumen: Sustainability promotion and resource conservation. *Resour., Conserv. Recycl.* **2021**, *171*, No. 105626.
(13) Dong, Z.; Zhou, T.; Luan, H.; Wang, H.; Xie, N.; Xiao, G.-q. Performance evaluation of bio-based asphalt and asphalt mixture and effects of physical and chemical modification. *Road Mater. Pavement Des.* **2020**, *21*, 1470−1489.
(14) Zhou, T.; Kabir, S. F.; Cao, L.; Luan, H.; Dong, Z.; Fini, E. H. Comparing effects of physisorption and chemisorption of bio-oil onto rubber particles in asphalt. *J. Cleaner Prod.* **2020**, *273*, No. 123112.
(15) Yang, X.; You, Z.; Dai, Q.; Mills-Beale, J. Mechanical performance of asphalt mixtures modified by bio-oils derived from waste wood resources. *Constr. Build. Mater.* **2014**, *51*, 424−431.
(16) Zhang, R.; You, Z.; Wang, H.; Chen, X.; Si, C.; Peng, C. Using bio-based rejuvenator derived from waste wood to recycle old asphalt. *Constr. Build. Mater.* **2018**, *189*, 568−575.
(17) Cao, Z.; Huang, X.; Yu, J.; Han, X.; Wang, R.; Li, Y. Laboratory evaluation of the effect of rejuvenators on the interface performance of rejuvenated SBS modified bitumen mixture by surface free energy method. *Constr. Build. Mater.* **2021**, *271*, No. 121866.
(18) Cao, Z.; Huang, X.; Yu, J.; Han, X.; Wang, R.; Li, Y. Study on all-components regeneration of ultraviolet aged SBS modified asphalt for high-performance recycling. *J. Cleaner Prod.* **2020**, *276*, No. 123376.
(19) Samieadel, A.; Islam Rajib, A.; Phani Raj Dandamudi, K.; Deng, S.; Fini, E. H. Improving recycled asphalt using sustainable hybrid rejuvenators with enhanced intercalation into oxidized asphaltenes nanoaggregates. *Constr. Build. Mater.* **2020**, *262*, No. 120090.
(20) Zadshir, M.; Hosseinnezhad, S.; Fini, E. H. Deagglomeration of oxidized asphaltenes as a measure of true rejuvenation for severely aged asphalt binder. *Constr. Build. Mater.* **2019**, *209*, 416−424.
(21) Zadshir, M.; Oldham, D. J.; Hosseinnezhad, S.; Fini, E. H. Investigating bio-rejuvenation mechanisms in asphalt binder via laboratory experiments and molecular dynamics simulation. *Constr. Build. Mater.* **2018**, *190*, 392−402.
(22) Cavalli, M. C.; Zaumanis, M.; Mazza, E.; Partl, M. N.; Poulikakos, L. D. Effect of ageing on the mechanical and chemical properties of binder from RAP treated with bio-based rejuvenators. *Composites, Part B* **2018**, *141*, 174−181.
(23) Yan, K.; Lan, H.; Duan, Z.; Liu, W.; You, L.; Wu, S.; Miljković, M. Mechanical performance of asphalt rejuvenated with various vegetable oils. *Constr. Build. Mater.* **2021**, *293*, No. 123485.
(24) Cao, X.; Wang, H.; Cao, X.; Sun, W.; Zhu, H.; Tang, B. Investigation of rheological and chemical properties asphalt binder rejuvenated with waste vegetable oil. *Constr. Build. Mater.* **2018**, *180*, 455−463.
(25) Fini, E.; Rajib, A. I.; Oldham, D.; Samieadel, A.; Hosseinnezhad, S. Role of Chemical Composition of Recycling Agents in Their Interactions with Oxidized Asphaltene Molecules. *J. Mater. Civ. Eng.* **2020**, *32*, No. 04020268.
(26) Zaumanis, M.; Mallick, R. B.; Poulikakos, L.; Frank, R. Influence of six rejuvenators on the performance properties of Reclaimed Asphalt Pavement (RAP) binder and 100% recycled asphalt mixtures. *Constr. Build. Mater.* **2014**, *71*, 538−550.
(27) Kecheng, Z.; Yuhong, W.; Yu, C.; Kaoqu, H. Effects of rejuvenators on relative molecular mass and size distribution of asphalt binders. *J. Build. Mater.* **2020**, *23*, 1130−1136.
(28) Rajib, A. I.; Samieadel, A.; Zalghout, A.; Kaloush, K. E.; Sharma, B. K.; Fini, E. H. Do all rejuvenators improve asphalt performance? *Road Mater. Pavement Des.* **2022**, 1−19.
(29) Ding, H.; Wang, H.; Qu, X.; Varveri, A.; Gao, J.; You, Z. Towards an understanding of diffusion mechanism of bio-rejuvenators in aged asphalt binder through molecular dynamics simulation. *J. Cleaner Prod.* **2021**, *299*, No. 126927.
(30) Li, R.; Bahadori, A.; Xin, J.; Zhang, K.; Muhunthan, B.; Zhang, J. Characteristics of bioepoxy based on waste cooking oil and lignin and its effects on asphalt binder. *Constr. Build. Mater.* **2020**, *251*, No. 118926.
(31) Li, L.; Xin, C.; Guan, M.; Guo, M. Using Molecular Dynamics Simulation to Analyze the Feasibility of Using Waste Cooking Oil as an Alternative Rejuvenator for Aged Asphalt. *Sustainability* **2021**, *13* (), DOI: 10.3390/su13084373.
(32) Jiang, X.; Li, P.; Ding, Z.; Wang, A.; Bing, H.; Zhang, J. Thermochemical liquefaction of wheat straw and its effectiveness as an extender for asphalt binders: Characterization of liquefied products and potential opportunities. *Constr. Build. Mater.* **2021**, *305*, No. 124769.
(33) Lei, Y.; Wang, H.; Chen, X.; Yang, X.; You, Z.; Dong, S.; Gao, J. Shear property, high-temperature rheological performance and low-temperature flexibility of asphalt mastics modified with bio-oil. *Constr. Build. Mater.* **2018**, *174*, 30−37.
(34) Lei, Y.; Wang, H.; Fini, E. H.; You, Z.; Yang, X.; Gao, J.; Dong, S.; Jiang, G. Evaluation of the effect of bio-oil on the high-temperature performance of rubber modified asphalt. *Constr. Build. Mater.* **2018**, *191*, 692−701.
(35) Zhang, R.; You, Z.; Wang, H.; Ye, M.; Yap, Y. K.; Si, C. The impact of bio-oil as rejuvenator for aged asphalt binder. *Constr. Build. Mater.* **2019**, *196*, 134−143.
(36) Yang, T.; Chen, M.; Zhou, X.; Xie, J. Evaluation of Thermal-Mechanical Properties of Bio-Oil Regenerated Aged Asphalt. *Materials* **2018**, *11*, 2224.
(37) Kabir, S. F.; Mousavi, M.; Fini, E. H. Selective adsorption of bio-oils' molecules onto rubber surface and its effects on stability of rubberized asphalt. *J. Cleaner Prod.* **2020**, *252*, No. 119856.
(38) Mokhtari, A.; David Lee, H.; Williams, R. C.; Guymon, C. A.; Scholte, J. P.; Schram, S. A novel approach to evaluate fracture surfaces of aged and rejuvenator-restored asphalt using cryo-SEM and image analysis techniques. *Constr. Build. Mater.* **2017**, *133*, 301−313.
(39) Martín-Martínez, F. J.; Fini, E. H.; Buehler, M. J. Molecular asphaltene models based on Clar sextet theory. *RSC Adv.* **2015**, *5*, 753−759.
(40) Li, D. D.; Greenfield, M. L. Chemical compositions of improved model asphalt systems for molecular simulations. *Fuel* **2014**, *115*, 347−356.
(41) Pahlavan, F.; Hung, A. M.; Zadshir, M.; Hosseinnezhad, S.; Fini, E. H. Alteration of π-Electron Distribution To Induce Deagglomeration in Oxidized Polar Aromatics and Asphaltenes in an Aged Asphalt Binder. *ACS Sustainable Chem. Eng.* **2018**, *6*, 6554−6569.
(42) Ungerer, P.; Rigby, D.; Leblanc, B.; Yiannourakou, M. Sensitivity of the aggregation behaviour of asphaltenes to molecular weight and structure using molecular dynamics. *Mol. Simul.* **2014**, *40*, 115−122.
(43) Xinheng, C.; Jun, L. O. N. G.; Qiang, R. E. N.; Ming, D. O. N. G.; Wei, W. A. N. G.; Songbai, T. I. A. N.; Zelong, L. I. U. Aggregation Mechanism of Asphaltene Molecular Aggregates. *Acta Pet. Sin.* **2019**, *35*, 920−928.
(44) Ren Qiang, L. J.; Zhenyu, D. A. I.; Han, Z. H. O. U. Theoretical study on π-π interactions in asphaltene molecular aggregate. *Acta Pet. Sin., Pet. Process. Sect.* **2019**, *35*, 751−758.
(45) Zhao, K.; Wang, Y.; Chen, L.; Li, F. Diluting or dissolving? The use of relaxation spectrum to assess rejuvenation effects in asphalt recycling. *Constr. Build. Mater.* **2018**, *188*, 143−152.
(46) Farrar, M. J.; Turner, T. F.; Planche, J.-P.; Schabron, J. F.; Harnsberger, P. M. Evolution of the Crossover Modulus with Oxidative Aging. *Transp. Res. Rec. J. Transp. Res. Board* **2013**, *2370*, 76−83.
(47) Mullins, O. C.; Sabbah, H.; Eyssautier, J.; Pomerantz, A. E.; Barré, L.; Andrews, A. B.; Ruiz-Morales, Y.; Mostowfi, F.; McFarlane,

R.; Goual, L.; Lepkowicz, R.; Cooper, T.; Orbulescu, J.; Leblanc, R. M.; Edwards, J.; Zare, R. N. Advances in Asphaltene Science and the Yen−Mullins Model. *Energy Fuels* **2012**, *26*, 3986−4003.
(48) Mousavi, M.; Hosseinnezhad, S.; Hung, A. M.; Fini, E. H. Preferential adsorption of nickel porphyrin to resin to increase asphaltene precipitation. *Fuel* **2019**, *236*, 468−479.
(49) Laukkanen, O.-V.; Pellinen, T.; Makowska, M. Exploring the Observed Rheological Behaviour of In-Situ Aged and Fresh Bitumen Employing the Colloidal Model Proposed for Bitumen. *Multiscale Model. Charact. Infrastruct. Mater.* **2013**, 185−197.
(50) Liu, F.; Zhou, Z.; Zhang, X.; Wang, Y. On the linking of the rheological properties of asphalt binders exposed to oven aging and PAV aging. *Int. J. Pavement Eng.* **2021**, *22*, 331−340.
(51) Oldham, D.; Qu, X.; Wang, H.; Fini, E. H. Investigating Change of Polydispersity and Rheology of Crude Oil and Bitumen Due to Asphaltene Oxidation. *Energy Fuels* **2020**, *34*, 10299−10305.
(52) Pahlavan, F.; Hung, A.; Fini, E. H. Evolution of molecular packing and rheology in asphalt binder during rejuvenation. *Fuel* **2018**, *222*, 457−464.
(53) Pahlavan, F.; Hosseinnezhad, S.; Samieadel, A.; Hung, A.; Fini, E. Fused Aromatics To Restore Molecular Packing of Aged Bituminous Materials. *Ind. Eng. Chem. Res.* **2019**, *58*, 11939−11953.
(54) Mousavi, M.; Pahlavan, F.; Oldham, D.; Abdollahi, T.; Fini, E. H. Alteration of intermolecular interactions between units of asphaltene dimers exposed to an amide-enriched modifier. *RSC Adv.* **2016**, *6*, 53477−53492.
(55) Eyring, H. Viscosity, Plasticity, and Diffusion as Examples of Absolute Reaction Rates. *J. Chem. Phys.* **1936**, *4*, 283−291.
(56) Jamshidi, A.; Hamzah, M. O.; Shahadan, Z.; Yahaya, A. S. Evaluation of the Rheological Properties and Activation Energy of Virgin and Recovered Asphalt Binder Blends. *J. Mater. Civ. Eng.* **2015**, *27*, No. 04014135.
(57) Hung, A. M.; Fini, E. H. Absorption spectroscopy to determine the extent and mechanisms of aging in bitumen and asphaltenes. *Fuel* **2019**, *242*, 408−415.

https://doi.org/10.1021/acsomega.2c01810
ACS Omega 2022, 7, 21736−21749